UCRL-10629 Rev.

University of California

Ernest O. Lawrence Radiation Laboratory

POLARIZATION OF RECOIL PROTONS IN $\pi^{\pm}p$ ELASTIC SCATTERING NEAR 600 MeV

TWO-WEEK LOAN COPY

This is a Library Circulating Copy which may be borrowed for two weeks. For a personal retention copy, call Tech. Info. Division, Ext. 5545

Berkeley, California

DISCLAIMER

This document was prepared as an account of work sponsored by the United States Government. While this document is believed to contain correct information, neither the United States Government nor any agency thereof, nor the Regents of the University of California, nor any of their employees, makes any warranty, express or implied, or assumes any legal responsibility for the accuracy, completeness, or usefulness of any information, apparatus, product, or process disclosed, or represents that its use would not infringe privately owned rights. Reference herein to any specific commercial product, process, or service by its trade name, trademark, manufacturer, or otherwise, does not necessarily constitute or imply its endorsement, recommendation, or favoring by the United States Government or any agency thereof, or the Regents of the University of California. The views and opinions of authors expressed herein do not necessarily state or reflect those of the United States Government or any agency thereof or the Regents of the University of California.

Submitted for publication in Physical Review

UCRL-10629 Rev.

UNIVERSITY OF CALIFORNIA

Lawrence Radiation Laboratory
Berkeley, California

AEC Contract No. W-7405-eng-48

POLARIZATION OF RECOIL PROTONS IN $\pi^{\pm}p$ ELASTIC SCATTERING NEAR 600 MeV*

Richard D. Eandi, Thomas J. Devlin,† Robert W. Kenney
Paul G. McManigal,‡ and Burton J. Moyer

May 21, 1964

POLARIZATION OF RECOIL PROTONS IN $\pi^{\pm}p$ ELASTIC SCATTERING NEAR 600 MeV*

Richard D. Eandi, Thomas J. Devlin,† Robert W. Kenney
Paul G. McManigal,‡ and Burton J. Moyer

Lawrence Radiation Laboratory
University of California
Berkeley, California

May 21, 1964

ABSTRACT

Angular distributions of recoil-proton polarization in elastic $\pi^{\pm}p$ scattering were measured at 523, 572, and 689 MeV incident pion kinetic energy. Polarization measurements were made by observing the azimuthal asymmetry in the subsequent scattering of recoil protons in large carbon-plate spark chambers. Typical strong variation of the polarization with pion scattering angle near the πp diffraction minima was observed. Since existing opinion favors a D_{13} resonance at 600 MeV, a phase shift analysis was attempted in order to confirm the existence and parity of this resonance. Available πp total and differential cross sections, these polarization data, and some possible restrictive assumptions related to the 600 MeV resonance were used in the analysis. Though the polarization results aided significantly in restricting the number of acceptable phase shift sets, still, many plausible and qualitatively different sets were found.

I. INTRODUCTION

Present knowledge of the natures of the various maxima occuring in the pion-nucleon cross sections,[1,2] for pion kinetic energies below 1.6 BeV (lab), includes quite certain assignments of angular momenta. Parities are, however, not confidently understood except in the well-known case of the "P_{33}" resonance (isotopic spin T = 3/2, angular momentum J = 3/2), occurring in pion scattering at 200 MeV kinetic energy in the laboratory frame, or 1238 MeV total energy in the πN center-of-mass frame.

Angular distribution in photoproduction[3,4,5] and in elastic scattering[6,7] have allowed assignments of angular momentum to the phenomena here of interest as follows:[8]

Isotopic Spin	Pion K. E. (Lab)	πN Total c.m. energy	J
3/2	200 MeV	1238 MeV	3/2
1/2	600 MeV	1512 MeV	3/2
1/2	900 MeV	1688 MeV	5/2
3/2	1350 MeV	1920 MeV	7/2

Our particular concern in this article is the phenomenon at 1512 MeV c.m. energy. Angular distribution measurements[8] infer that a J = 3/2 amplitude is strong at this energy; but other amplitudes are not small, so that it is difficult to conclude that the behavior in this region is simply due to a single state in resonance. This observation is expressed also by those performing recent photoproduction measurements through this energy range.[9]

Peierls' early speculative assignment[3] of a "$D_{3/2}$ resonance" at this energy is still tentatively retained. In fact it is supported by experimental measurements of proton recoil polarization in photoproduction experiments in the energy regions immediately below[10,11] and above[12] the 1512 MeV position, as interpreted after the theoretical arguments of Sakurai,[13] and Moravcsik,[14] and of Shaw.[15] But recent recognition of the plurality of significantly strong

amplitudes in this region[9,16] makes it desirable to test the uniqueness of the $D_{3/2}$ assignment. In particular, in view of the Minami ambiguity,[17] we here investigate whether or not a $P_{3/2}$ assignment could be compatible with angular distributions and polarization measurements obtained in elastic πN scattering through the region containing the 1512 MeV phenomenon.

II. EXPERIMENTAL METHOD

A measurement of the polarization of the recoil proton in πp scattering requires that one look for an azimuthal asymmetry in a subsequent scattering of the proton by a suitable polarization analyzer. From the conservation of parity in strong interactions it can be shown that the proton polarization is perpendicular to the plane of scattering. The magnitude of the polarization, P, is determined from the angular distribution of the recoil proton scattered by the analyzer according to the expression[18]

$$\sigma(\theta,\emptyset,T) = \sigma_o(\theta,T)\ [1 + PA(\theta,T)\cos\emptyset]$$

where $A(\theta,T)$ is the analyzing power of the second scatterer for collisions in which protons of energy T are deflected through an angle θ, $\emptyset$ is the azimuthal angle between planes of the first and second scatter, and σ_o is the cross section for unpolarized protons.

In this experiment, two carbon-plate spark chambers were used as analyzer-detectors. Their high angular resolution and wide angular acceptance, sharp energy resolution, and large sensitive volume allowed the simultaneous measurement of recoil proton polarization over a wide angular range. The spark chambers were triggered by an array of scintillation and Cerenkov counters which identified the particle entering the chambers as recoil protons from elastic pion-proton scattering.

The experimental set up is shown in Fig. 1. The pions were produced by bombarding an aluminum oxide ceramic target with the circulating beam of

protons in the Bevatron. The pions traversed the apparatus of another experiment[8] and were refocused by means of a quadrupole on our target. The central momentum, the momentum spread ($\Delta P/P = \pm 3\%$), and the composition of the beam were determined by a magnetic beam-transport system of this upstream experiment. The pion beam was monitored by counters M_1, M_2, and M_3 before entering the hydrogen target. A1 and A2 were annular anti-coincidence counters for further defining the pion beam. Each spark chamber had four identical channels (distributed in azimuthal angle, although only one can be illustrated in Fig. 1) each consisting of a pion counter $\pi(i)$, a proton counter $p(i)$ ($i = 1, 2, 3, 4$) and a Cerenkov counter, C. Each channel selected elastic scattering events by imposing the condition that the incident pion and the two scattered particles be coplanar. To insure that only protons entered the chambers, the scattered pion was detected by a water Cerenkov counter which would not respond to protons. The kinematically conjugate counter was then assumed to count the recoil proton. Recoil protons scattering from the hydrogentarget with their polar angle between 13 and 40-deg were detected by chamber A; angles between 32 and 65 deg by chamber B.

The electronic logic arrays used to trigger the chambers were identical. Either chamber was triggered on the following signature: $M_1M_2M_3C\bar{A}_1\bar{A}_2p(i)\pi(i)$. The selection of events other than elastic π-p scattering was minimized by this multiplicity of the coincidence and the stringent coplanarity requirement. The effect of the inelastic background was made insignificant by imposing range requirements on the recoil proton consistent with kinematics for elastic scattering. The ratio of target-full to target-empty counting rate was 20 or greater. The effect of background was all but eliminated by requiring in the film scanning that the particle track, in addition to range requirements, must have its origin in the liquid target when projected back along its direction of flight.

III. DATA ANALYSIS

The calculation of the polarization of recoil protons scattering into a given angular interval was performed in two steps.

First, the spark chamber film was scanned and each selected scatter was geometrically and kinematically reconstructed. For each of the two orthogonal views, the proton-carbon scattering angle and sense, the number of carbon plates traversed by the proton before scattering, and the total number of plates traversed before stopping were recorded. From this recorded information the energy T, scattering angle θ, and azimuthal angle $\emptyset$ were computed for each selected p-C scatter. Second, the polarization for a given pion scattering angle was then estimated by grouping all the corresponding recoil protons and applying the maximum likelihood method to this event sample. The maximum likelihood theorem[20] states that the value of P is that value which allows the observed array of events in the sample to be consistent with maximum probability and thereby maximizes the expression

$$L(P) = \prod_{i}^{\text{events}} \left[1 + PA(\theta_i, T_i) \cos \emptyset_i\right] .$$

The statistical error is arbitrarily defined as that increment of P which makes L/L_{max} equal to $e^{-1/2}$.

The determination of $A(T,\theta)$ was limited by the momentum resolution of the beam transport system, and by the one inch thickness of the carbon plates. This limited our ability to determine the elasticity of a given p-C scatter. In our case the energy resolution, determined by investigating the energy distribution of the accepted events about the kinematically calculated recoil proton energy, was 30 MeV. To compensate for this effect, we used[19] a modified analyzability which was a function of proton energy and angle; this includes the effect of inelastic scatters with energy losses of up to 30 MeV.

This modified analyzability is reproduced in the form of a normalized contour map in Figs. 2 and 3. Events having a p-C scattering angle below $\theta(T/180\ \mathrm{MeV})^{1/2} = 4$ deg and above $\theta(T/180\ \mathrm{MeV})^{1/2} = 24$ deg were rejected. This insured that for the proton-energy interval covered, the p-C analyzability does not change sign. Thus a propensity to scatter to the left (looking parallel to the particle path) in the chamber always meant a positive (upward) polarization. This is consistent with the convention that the polarization is positive in the direction $(\vec{P}_i \times \vec{P}_f)$ where $\vec{P}_i$ and $\vec{P}_f$ are the initial and final pion momenta, respectively.

The average detection efficiencies were measured separately for left and right scattering by comparison of the same film scanned by different scanners. Also a portion of the film was reversed such that left-right appeared right-left and rescanned. The left and right efficiencies determined by this repeated scanning were found to be the same within statistics. No significant asymmetry normal to the πp scattering plane was found for the accepted p-C events. Bias effects are concluded negligible in comparison to the large inherent statistical uncertainty. The uncertainty in the polarization resulting from the uncertainty in the analyzing power can be obtained by investigating the changes in the calculated polarization when the analyzability is modified within the limits of the error $A(T,\theta)$ obtained from p-C scattering experiments. Thus the parameter $A(T,\theta)$ was altered $\pm$ 0.05, corresponding to the average empirical uncertainty of the p-C scattering experiments, and the polarization recalculated. The deviation from quoted values depended on the make-up of the sample. Average deviation in polarization was 0.03. This test of sensitivity of the data due to a systematically high or low analyzability gives an upper limit of the possible deviation in polarization, since it is highly unlikely that the p-C scattering measurements are either all high or all low.

Table I gives the resulting polarization $P(\cos\theta^*_\pi)$ determined in this experiment for 523, 572, and 689 MeV, incident pion energy.

IV. DISCUSSION OF RESULTS

It is well known that the product of the polarization and the differential cross section at a given energy can be written as a power series in $\cos\theta^*_\pi$:

$$\frac{P(\theta^*_\pi)\,\sigma(\theta^*_\pi)}{\sin\theta^*_\pi} = \sum^{2(\ell_{max})-1} b_n \cos^n\theta^*_\pi \quad ,$$

where the b's are linear combinations of products between partial-wave amplitudes, and ℓ_{max} is the state of maximum angular momentum involved in the scattering.[14] A least-squares fit was made of this cosine power series to the polarization data. The series was terminated by applying standard statistical tests. The results are given in Tables II and III. These tables show that the statistical accuracy of the data of this experiment is unable to resolve the presence or absence of the higher angular momentum states which manifest themselves in the coefficients of higher powers of $\cos\theta^*_\pi$. The lower order coefficients, b_0 and b_1, are reliably determined, because they did not deviate in magnitude or sign as we increased the order of fit. However b_3 and b_4 tended to depend significantly on the order of fit. This is reflected in the large errors of these coefficients. Also the inclusion of higher order coefficients permitted least-square fits which were unphysical in that they predicted the polarization in the angular region where no polarization data exist to be significantly greater than one. This symptom is due to the inability of the present data to determine the higher order coefficients.

If we accept the results of Table II, then the failure of particular coefficients to dominate the expansion indicates that a large number of states must contribute. If there is one angular momentum state which really dominates

in this energy region, its presence is hidden by its interference with the numerous other states. This is confirmed by angular-distribution and photoproduction experiments.[4,5,9] Therefore, the assumption that the πN interaction at these energies is dominated by the influence of neighboring single-state resonances as proposed by Moravcsik[14] is unfortunately oversimplified.

In order to circumvent the above problem, a method of analysis is needed which: first, inherently contains the condition that the polarization is bounded by unity, and second, makes use of other independent data to further constrain the polarization in the angular region where no polarization data exist. The conventional method for doing this is phase shift analysis, for this technique provides a simultaneous least squares fit of all the available data at a given energy.

Since scattering experiments[8] indicate that no angular momentum states higher than $\ell = 3$ contribute significantly at energies below 1 BeV, an attempt was made to use total[2] and differential[8] cross sections and the forward scattering amplitude,[21] as well as polarization, in order to obtain a best fit to all the observables simultaneously by expressing these observables in terms of a basic set of partial waves.[22] This was accomplished by using a computer to search for sets of amplitudes that agree with all the existing data. Sets of phase shifts were obtained for each of the three energies by feeding random sets of phase shifts as input to the computer, then allowing the computer to converge on a best fit. Many phase shift sets were found. A large number of these solutions gave sets of phase shifts which differed qualitatively from one another. Based upon the data used, the attainment of a unique phase shift solution was impossible.

But since existing data[2,3] favor a resonance having the quantum numbers $J = 3/2$, $T = 1/2$, and either even or odd parity at 600 MeV, a less ambitious attempt was made to find a set of phase shifts at 523, 572, and 689

MeV that would satisfy the following restrictive assumptions, where (a) and (b) under 2 are alternative choices.

1. The phase shift sets at the three energies must be consistent among themselves and agree with the lower-energy phase shifts.[23] This demands that the value of the phase shift for each state must vary smoothly with energy, as expected from causality.

2. (a) A D-wave, iso-spin 1/2, angular momentum 3/2, highly absorptive resonance exists at 600 MeV.

(b) A P_{13} rather than a D_{13} resonance exists at 600 MeV.

The two states [2 (a) and (b)] have the same angular distribution and total cross section since they possess the same J value (Minami ambiguity). Thus with the inclusion of the polarization data of this experiment, we hoped to satisfy either one set of assumptions or the other, and thereby resolve the parity of the resonant state. It must be remembered that phase shifts that satisfy one of the above sets of restrictions would be only a plausible, nonunique solution to the problem. Nevertheless, it would establish that all the available $\pi^{\pm}p$ data are consistent with either a P_{13} resonant state as predicted by Wilson,[24] or a D_{13} resonant state as predicted by Peierls.[3]

With this in mind, we introduced sets of phase shifts favoring the D_{13} case to the computer as input information. The computer was then permitted to vary all the phase shifts and obtain solutions at each energy which one hoped would preserve the qualitative behavior of the original input set. The same procedure was followed for the P_{13} case. A consistent and plausible set of phase shifts was found at each energy for both cases; these are given in Table IV. Table V gives the pertinent information concerning the best-fit criteria. Values of the coefficients of the cosine power series for polarization and differential cross sections, calculated from these phase shifts, are tabulated in Table VI. The polarization coefficients for both cases, the

P and D resonance possibilities, are essentially the same as the b's obtained by fitting just the polarization data (Table II). Any differences may be explained by the additional constraints imposed upon the polarization in the angular region where no polarization data exist. The differential-cross-section coefficients are in essential agreement with Helland et al.,[8] whose coefficients were obtained by fitting only angular distribution data.

Qualitatively, the phase shift sets for both cases have a reasonable behavior with respect to incident-pion energy. The strong S- and P-wave absorption in the T = 1/2 channel is consistent with the behavior of the cross section for pion production observed at these and lower energies.[25] The only significant departure in their behavior is in the phase shift for the J = 3/2, T = 1/2 P- or D-wave state, which possesses an assumed resonant behavior at 600 MeV. That both cases agree with the abundant $\pi^{\pm}p$ data available is an indication that the accuracy of the polarization data must be improved before the parity of the given state can be determined. Although the D_{13} case is favored by the various πN and $\pi\pi$ isobar models proposed by Peierls[26] and Ball and Frazer[27] to explain the higher-energy maxima, the statistical accuracy of the polarization data measured in this experiment cannot resolve the two cases. This is most strikingly seen in Fig. 4, where the computed curves for both cases are presented.

Figures 5 and 6 show charge exchange polarization and differential cross sections computed from the phase shift sets given in Table IV. It appears that the charge exchange differential cross section is insensitive to a resonance in either the D_{13} or P_{13} partial wave at 600 MeV. On the other hand the charge exchange recoil neutron polarization appears to be quite sensitive to the parity of the resonance. However, this distinctive behavior of the neutron polarization may be due to the qualitatively different behavior of other background partial waves rather than to whether the resonance is

D_{13} or P_{13}. In any case, more experimental information, especially recoil proton polarization with smaller errors and recoil neutron polarization in charge exchange, is clearly needed in order to ultimately solve for a unique set of angular momentum amplitudes that would completely determine πN scattering at these energies.

ACKNOWLEDGEMENTS

We thank Professor V. Z. Peterson for his valuable discussions on how to make optimum use of existing p-C polarization data in order to determine the polarization of incident protons on carbon. We are grateful to Professor Robert J. Cence for the use of his phase shift search program and for the many useful discussions on the problems of phase shift analysis. We thank Dr. Jerome A. Helland for providing the pion beam; his complete cooperation in the simultaneous use of the beam is gratefully acknowledged.

FOOTNOTES AND REFERENCES

* This work was supported by the U. S. Atomic Energy Commission.

† Present address: Princeton University, Princeton, New Jersey.

‡ Present address: Aeronutronic Division, Ford Motors, Newport Beach, California

1. J. C. Brisson, J. F. Detoeuf, P. Falk-Vairant, L. van Rossum, and G. Valladas, Nuovo Cimento 19, 210 (1961).

2. Thomas J. Devlin, Burton J. Moyer, and Victor Perez-Mendez, Phys. Rev. 125, 690 (1962).

3. Ronald F. Peierls, Phys. Rev. 118, 325 (1960).

4. F. P. Dixon and R. L. Walker, Phys. Rev. Letters 1, 458 (1958).

5. J. I. Vette, Phys. Rev. 111, 622 (1958).

6. Burton J. Moyer, Rev. Mod. Phys. 33, 367 (1961).

7. Jerome A. Helland, Thomas J. Devlin, Donald E. Hagge, Michael J. Longo, Burton J. Moyer, and Calvin D. Wood, Phys. Rev. Letters 10, 27 (1963).

8. a. Jerome A. Helland, Calvin D. Wood, Thomas J. Devlin, Donald E. Hagge, Michael J. Longo, Burton J. Moyer, and Victor Perez-Mendez, "Elastic Scattering of Negative Pions on Protons in Energy Range 500 to 1000 MeV." (To be published in Phys. Rev.)

   b. Jerome A. Helland, Thomas J. Devlin, Donald E. Hagge, Michael J. Longo, Burton J. Moyer and Calvin D. Wood. "Elastic Scattering of Positive Pions in the Energy Range 500 to 1600 MeV" (To be published in Phys. Rev.)

9. M. Beneventano, R. Finzi, L. Mezzetti, L. Paoluzi, and S. Tazzari, Nuovo Cimento 28, 1464-83, June 16, 1963.

10. J. O. Maloy, G. A. Salandin, A. Manfredini, V. Z. Peterson, J. I. Friedman, and H. Kendall, Phys. Rev. 122, 1338 (1961).

11. R. Querzoli, G. Salvini, and A. Silverman, Nuovo Cimento 19, 53 (1961).

12. C. Mancuccini, R. Querzoli, and G. Salvini, Phys. Rev. 126, 1181-2 (1962).

13. J. J. Sakurai, Phys. Rev. Letters 1,258 (1958).

14. Michael J. Moravcsik, Phys. Rev. 118, 1615 (1960).

15. Peter B. Shaw, Phys. Rev. 124, 1971 (1961).

16. Detailed elastic scattering measurements at Saclay by a collaboration of Saclay and Berkeley groups have indicated that a $D_{3/2}$ amplitude must be accompanied by a prominent $P_{1/2}$ and $D_{5/2}$ amplitudes. (To be published).

17. Shigeo Minami, Progr. Theoret. Phys. (Kyoto) 11, 213 (1954).

18. W. S. C. Williams, An Introduction to Elementary Particles, (Academic Press, Inc., New York, 1961) Chap. VIII.

19. Vincent Z. Peterson, Lawrence Radiation Laboratory Report UCRL-10622 (unpublished).

20. Harald Cramer, Mathematical Methods of Statistics, (Princeton University Press, Princeton, New Jersey, 1958) p. 498.

21. J. W.Cronin, Phys. Rev. 118, 824 (1960).

22. W. S. C. Williams, An Introduction To Elementary Particles, (Academic Press, Inc., New York, 1961) Chap. III.

23. Olav T. Vik and Hugo R. Rugge, Phys. Rev. 129, 2311 (1963).

24. Robert R. Wilson, Phys. Rev. 110, 1212 (1958).

25. Janos Kirz, Joseph Schwartz, and Robert D. Tripp, Phys. Rev. 130, 2481 (1963).

26. Ronald F. Peierls, Phys. Rev. Letters 6, 641 (1961).

27. James S. Ball and William R. Frazer, Phys. Rev. Letters 7, 204 (1961).

FIGURE CAPTIONS

1. Plan view of the experiment, showing the orientation of spark chambers and corresponding counters used to select desired events.

2. Curves of constant A^* for p-C scattering, corrected for the inclusion of inelastic scatterings with up to 30 MeV loss ($\Delta\epsilon$ = 30 MeV). The contours are displayed as a function of laboratory energy of the incident proton T, and angle θ^*. The parameters θ^* and A^* are related to laboratory p-C scattering angle θ_L and real p-C analyzability A by

$$\theta^* = \theta_L(T/180 \text{ MeV})^{1/2} \text{ and } A^* = A/A_{max} .$$

A_{max} is given in Fig. 3. The use of the starred variables helped remove predictable, strong variation of the analyzability.

3. Curve of A_{max} as a function of incident-proton kinetic energy. A_{max} is the largest magnitude the analyzability A ever attains between zero degrees and the first diffraction minimum for incoming protons of a given energy.

4. Differential polarization curves, computed by using the plausible phase shift sets given in Table IV, plotted along with the experimental data. The solid-line curves are those computed from phase shift set I consistent with a D_{13} resonance at 600 MeV. The dashed-line curves are computed from set II, consistent with a P_{13} resonance. If a dashed-line curve is not shown it means that for all practical purposes the two curves are the same.

5. Charge exchange ($\pi^- + p \rightarrow \pi^0 + n$) differential cross sections computed from the phase shift sets given in Table IV.

6. Differential polarization of the recoil neutron in the interaction $\pi^- + p \rightarrow \pi^0 + n$, computed from the phase shift sets given in Table IV.

Table I. Recoil-proton polarization for πN elastic scattering as a function of the cosine of c.m. pion scattering angle. The polarization values quoted were derived by using the effective p-C analyzing power given in Figs. 2 and 3. The errors quoted do not include the error in polarization resulting from uncertainty in analyzing power and systematic errors. (See Sec. III) Only the statistical uncertainty is shown, the other uncertainties being negligible.

π^+p		π^-p	
523 MeV		523 MeV	
Cos θ^*_π	Polarization	Cos θ^*_π	Polarization
+0.250±0.050	-0.26±0.32	+0.250±0.050	-0.94±0.26
+0.150±0.050	-0.34±0.19	+0.150±0.050	-0.94±0.20
+0.050±0.050	-0.42±0.17	+0.050±0.050	-0.34±0.20
-0.050±0.050	-0.44±0.20	-0.050±0.050	-0.02±0.24
-0.175±0.075	+0.20±0.28	-0.150±0.050	-0.78±0.28
-0.325±0.075	-0.56±0.30	-0.275±0.075	+0.38±0.20
-0.475±0.075	-0.10±0.34	-0.400±0.050	+0.42±0.26
-0.625±0.075	-0.36±0.17	-0.525±0.075	+0.10±0.16
-0.775±0.075	-0.14±0.21	-0.675±0.075	+0.10±0.10
		-0.825±0.075	-0.04±0.14
572 MeV		572 MeV	
Cos θ^*_π	Polarization	Cos θ^*_π	Polarization
+0.300±0.050	+0.14±0.26	+0.300±0.050	-0.56±0.36
+0.200±0.050	-0.12±0.16	+0.200±0.050	-0.26±0.24
+0.100±0.050	-0.22±0.16	+0.100±0.050	-0.58±0.19
0.000±0.050	-0.30±0.16	-0.025±0.075	-0.36±0.20
-0.100±0.050	-0.12±0.24	-0.175±0.075	-0.18±0.29
-0.225±0.075	+0.38±0.22	-0.300±0.050	+0.64±0.39
-0.375±0.075	+0.64±0.28	-0.400±0.050	+0.12±0.33
-0.525±0.075	+0.44±0.24	-0.500±0.050	-0.10±0.23
-0.650±0.050	+0.22±0.20	-0.600±0.050	-0.62±0.15
-0.775±0.075	-0.14±0.20	-0.700±0.050	-0.58±0.14
		-0.800±0.050	-0.38±0.19
689 MeV		689 MeV	
Cos θ^*_π	Polarization	Cos θ^*_π	Polarization
+0.375±0.075	-0.36±0.24	+0.350±0.050	-0.48±0.34
+0.250±0.050	-0.20±0.22	+0.250±0.050	-0.28±0.24
+0.150±0.050	-0.32±0.20	+0.150±0.050	-0.20±0.22
+0.025±0.075	-0.28±0.22	+0.050±0.050	-0.14±0.22
-0.125±0.075	+0.38±0.32	-0.050±0.050	+0.54±0.30
-0.275±0.075	+0.80±0.22	-0.175±0.075	+0.70±0.20
-0.425±0.075	+0.44±0.20	-0.325±0.075	+0.06±0.18
-0.575±0.075	+0.18±0.17	-0.450±0.050	+0.02±0.22
-0.725±0.075	+0.70±0.18	-0.550±0.050	-0.16±0.16
		-0.650±0.050	-0.44±0.16
		-0.750±0.050	-0.24±0.18

Table II. Coefficients b_n from the expansion $\frac{P(\theta)\sigma(\theta)}{\sin\theta} = \sum_{n=0}^{n} b_n \cos^n\theta$, obtained by fitting polarization data only

	Incident-pion energy (MeV)	b_0(mb)	b_1(mb)	b_2(mb)	b_3(mb)	b_4(mb)
	523	-0.143±0.039	-0.802±0.290	-1.570±0.093	-0.909±0.861	-
π^+p	572	-0.052±0.027	-0.307±0.189	-0.058-0.656	0.381±0.655	-
	689	0.003±0.027	-0.427±0.117	-0.940±0.555	-1.021±0.748	-
	523	-0.217±0.062	-1.674±0.347	-3.115±1.388	-1.795±1.537	-
π^-p	572	-0.179±0.043	-1.211±0.313	-0.809±1.278	2.397±1.479	-
	689	0.055±0.041	-0.910±0.308	-2.405±1.116	1.989±4.409	3.284±4.967

Table III. Values of χ^2 and $(\chi^2/D)^{1/2}$, and number of data points used for the order fit chosen.

	Incident-Pion energy (MeV)	No. of data points	Order of Fit, N	Degrees of freedom, D	χ^2	$(\chi^2/D)^{1/2}$
	523	9	3	5	6.00	1.10
π^+p	572	10	3	6	3.91	0.81
	689	9	3	5	7.41	1.22
	523	12	3	8	9.79	1.10
π^-p	572	11	3	7	4.83	0.83
	689	11	4	6	2.66	0.67

Table IV. Two plausible sets of phase shifts consistent with all the $\pi^{\pm}p$ total and differential cross sections, real part of forward scattering amplitude, and polarization data. Phase Shift Set I is consistent with a D_{13} resonant behavior at 600 MeV; Set II with a P_{13} resonance. Each set was obtained by starting the respective search with a set of initial phase shifts favoring the desired resonant behavior.

Set I

State	523 MeV		572 MeV		698 MeV	
$\ell_{2T,2J}$	δ(deg)	η	δ(deg)	η	δ(deg)	η
$S_{3,1}$	-22.6	0.82	-22.3	1.00	-16.6	1.00
$P_{3,1}$	- 1.9	0.83	- 6.7	0.79	- 9.1	0.65
$P_{3,3}$	155.2	1.00	159.3	1.00	159.7	0.97
$D_{3,3}$	4.6	0.98	2.8	0.98	- 4.0	0.85
$D_{3,5}$	- 9.4	0.94	- 8.0	0.89	0.8	0.93
$F_{3,5}$	- 1.0	1.00	0.6	1.00	2.5	0.95
$F_{3,7}$	0.6	1.00	3.5	0.98	1.8	0.96
$S_{1,1}$	- 2.4	0.25	-37.6	0.49	-42.4	0.71
$P_{1,1}$	6.1	0.52	21.6	0.71	16.7	0.54
$P_{1,3}$	0.6	1.00	- 3.0	1.00	-14.5	0.60
$D_{1,3}$	43.4	0.84	61.7	0.47	151.9	0.40
$D_{1,5}$	4.8	0.93	1.6	0.91	10.7	0.88
$F_{1,5}$	6.0	1.00	17.3	1.00	13.2	0.93
$F_{1,7}$	0.8	0.99	- 0.8	0.97	3.9	0.99

Set II

State	523 MeV		572 MeV		689 MeV	
$\ell_{2T,2J}$	δ(deg)	η	δ(deg)	η	δ(deg)	η
$S_{3,1}$	-21.8	0.81	-22.5	0.97	-16.9	1.00
$P_{3,1}$	- 1.0	0.84	- 7.0	0.80	- 6.5	0.64
$P_{3,3}$	155.2	0.99	158.4	0.98	159.2	0.94
$D_{3,3}$	4.9	0.99	2.5	1.00	- 3.6	0.86
$D_{3,5}$	- 9.9	0.94	- 7.4	0.89	0.1	0.94
$F_{3,5}$	- 1.0	1.00	- 0.8	1.00	2.9	0.97
$F_{3,7}$	0.4	1.00	3.1	1.00	1.5	0.96
$S_{1,1}$	32.6	0.05	7.5	0.18	-10.4	0.49
$P_{1,1}$	18.7	1.00	37.8	0.42	- 2.0	0.28
$P_{1,3}$	40.2	0.65	81.3	0.38	133.8	0.58
$D_{1,3}$	10.4	0.96	7.7	1.00	9.2	0.53
$D_{1,5}$	- 6.3	0.96	1.5	0.96	5.4	0.95
$F_{1,5}$	1.5	1.00	2.6	1.00	6.0	1.00
$F_{1,7}$	6.6	1.00	5.9	1.00	7.4	0.91

Table V. Values of χ^2 found for solutions in Table IV.

	523 MeV	572 MeV	689 MeV
Number of data points fitted, N[a]	53	57	58
Number of parameters varied[b]	28	28	28
χ^2, assuming D_{13} resonance	37	62	27
χ^2, assuming P_{13} resonance	38	54	27
Best χ^2 value ever attained, assuming no resonance[c]	37	55	27
χ^2 expected[d]	25	29	30

[a]Experimental data used, besides polarization, was taken from references 1, 2, 8, and 21.

[b]If we include up to $\ell = 3$, we have two spin orientations for each angular momentum state except $\ell = 0$, the real and imaginary parts of the phase shifts for each partial wave, and two possibilities for the value of the isotopic spin of each wave, giving a total of 28 independent parameters.

[c]This value is the best value of χ^2 obtained by looking at many phase shift sets obtained by random-search procedure.

[d]Here χ^2_{exp} means the number of degrees of freedom; that is, the number of experimental points fitted minus the number of phase shifts varied.

Table VI. Values of the coefficients a_n and b_n from the expansions

$$\sigma(\theta) = \lambda\!\!\!^{-2} \sum_n a_n \cos^n\theta \text{ and } \frac{P(\theta)\sigma(\theta)}{\sin\theta} = \lambda\!\!\!^{-2} \sum_n b_n \cos^n\theta$$

Calculated from Phase Shift Set I.

Coefficients[a]	523 MeV		572 MeV		689 MeV	
	π^+p	π^-p	π^+p	π^-p	π^+p	π^-p
a_0	0.21	0.18	0.18	0.17	0.11	0.14
a_1	0.97	0.67	0.94	0.92	0.54	0.60
a_2	1.33	1.02	1.48	1.78	1.58	2.55
a_3	-0.05	-0.06	-0.24	0.14	-0.16	-0.73
a_4	-0.44	0.33	-1.13	0.13	-1.83	-2.28
a_5	0.15	0.05	0.10	0.23	0.26	1.94
a_6	-0.00	0.00	0.30	0.08	0.86	1.75
b_0	-0.06	-0.09	-0.03	-0.06	-0.01	0.04
b_1	-0.30	-0.68	-0.17	-0.81	-0.30	-0.52
b_2	-0.48	-1.16	-0.04	-1.84	-0.38	-1.59
b_3	-0.16	-0.88	0.22	-1.28	-0.05	0.07
b_4	0.07	-0.36	0.03	-1.55	0.31	0.98
b_5	0.00	-0.04	-0.01	-0.62	0.01	0.34

Calculated from Phase Shift Set II.

Coefficients[a]	523 MeV		572 MeV		689 MeV	
	π^+p	π^-p	π^+p	π^-p	π^+p	π^-p
a_0	0.20	0.19	0.18	0.18	0.10	0.14
a_1	0.97	0.78	0.93	1.06	0.53	0.61
a_2	1.33	1.08	1.43	1.96	1.57	2.51
a_3	-0.04	-0.64	-0.20	-0.38	-0.11	-0.69
a_4	-0.43	0.05	-0.96	-0.35	-1.79	-2.33
a_5	0.14	0.58	0.10	0.57	0.21	1.84
a_6	-0.00	0.15	0.18	0.46	0.82	1.87
b_0	-0.06	-0.12	-0.03	-0.09	-0.01	0.03
b_1	-0.30	-0.77	-0.16	-0.69	-0.30	-0.55
b_2	-0.51	-0.92	-0.03	-0.77	-0.35	-1.52
b_3	-0.21	-0.06	0.21	0.76	0.03	0.77
b_4	0.04	0.15	0.04	-0.01	0.21	1.13
b_5	0.00	0.03	0.00	0.00	-0.19	-0.67

[a]To compare these coefficients with Table II the coefficients must be multiplied by $\lambda\!\!\!^{-2}$; $\lambda\!\!\!^{-2}$ = 2.21, 1.99, and 1.60 mb for T_π = 523, 572, and 689 MeV, respectively.

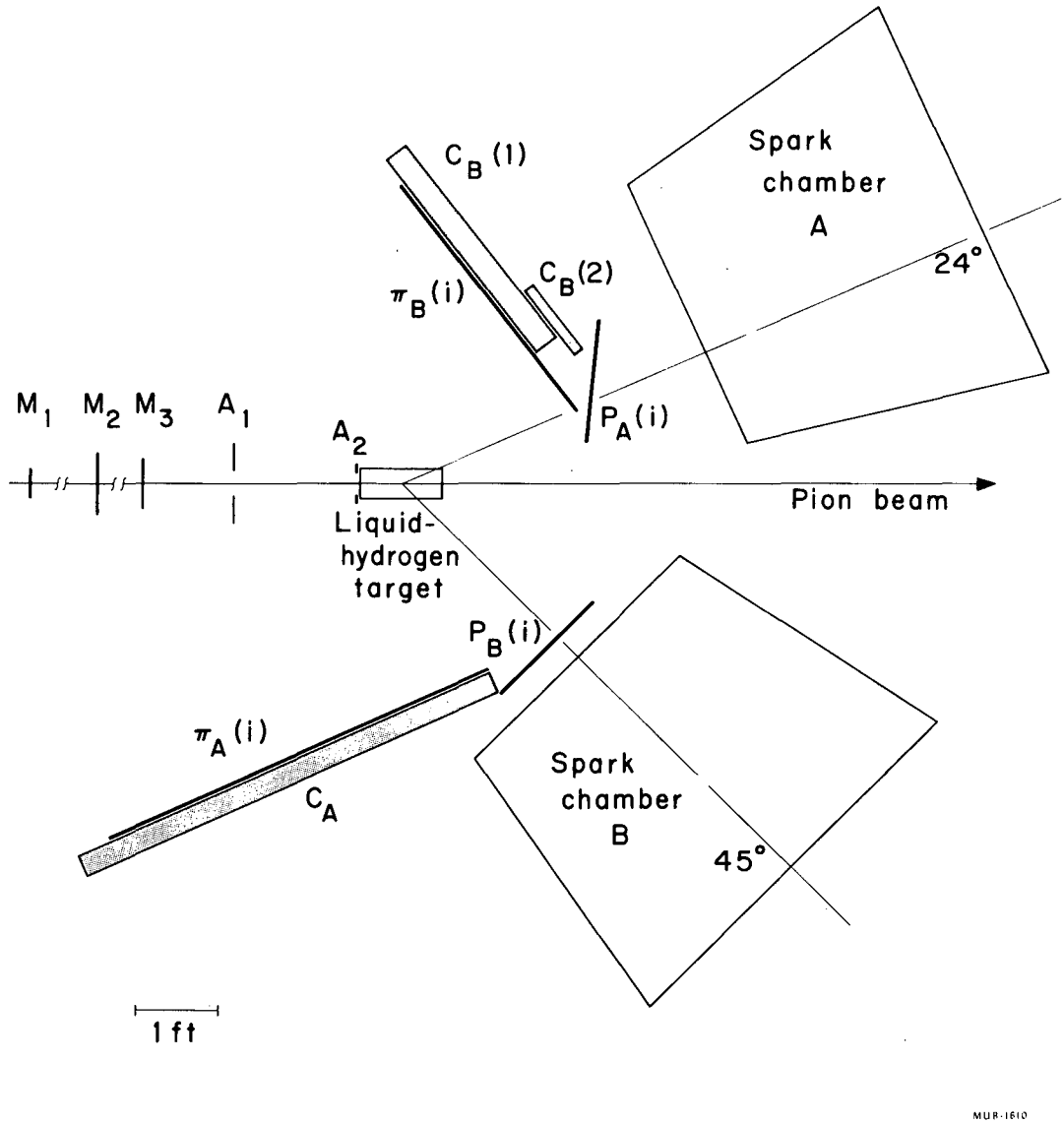
C_B (1)
Spark chamber A
24°
C_B(2)
π_B(i)
P_A(i)
M_1 M_2 M_3 A_1
A_2
Pion beam
Liquid-hydrogen target
P_B(i)
π_A(i)
C_A
Spark chamber B
45°
1 ft
MUR-1610

Fig. 1.

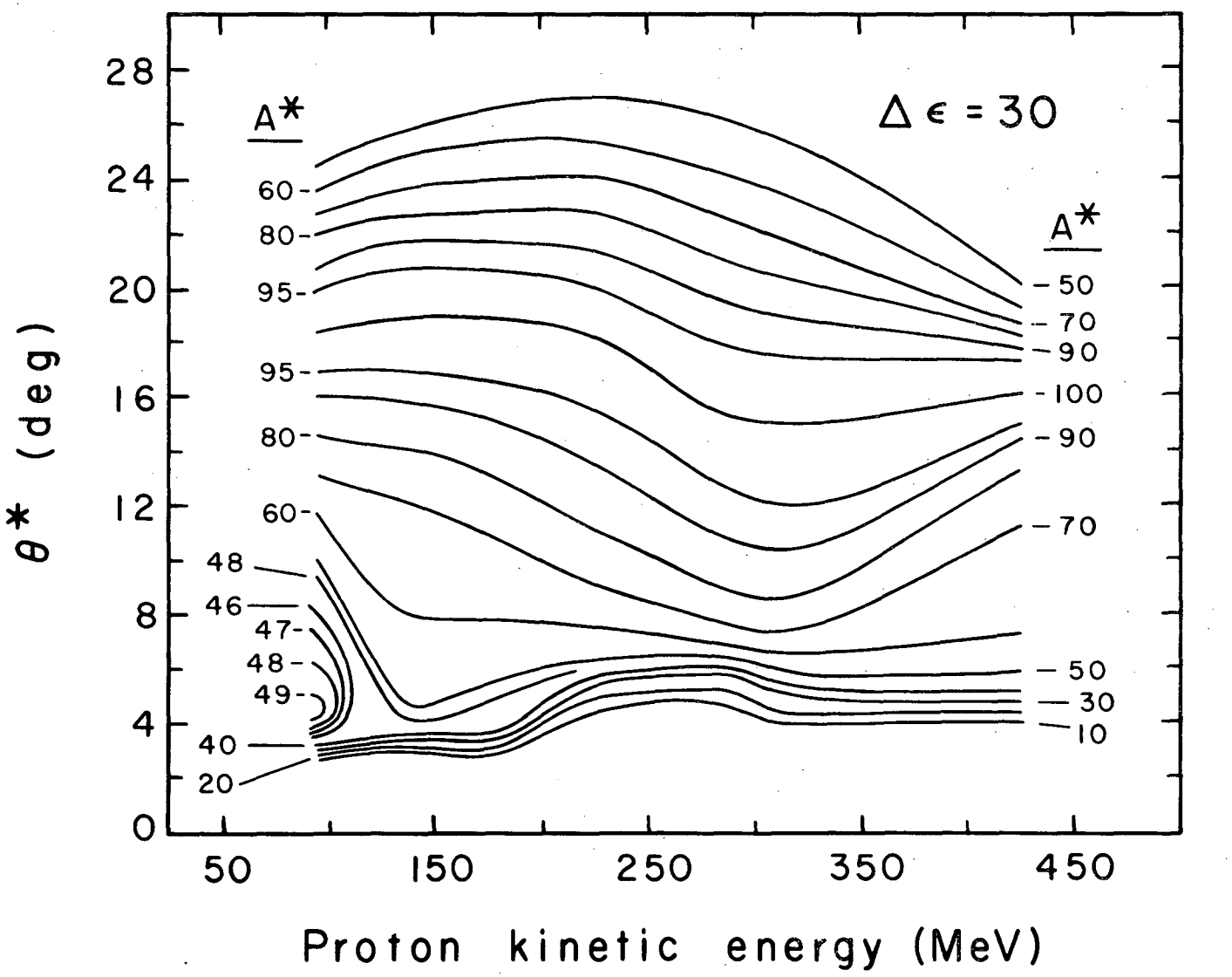

MU-29521-A

Fig. 2.

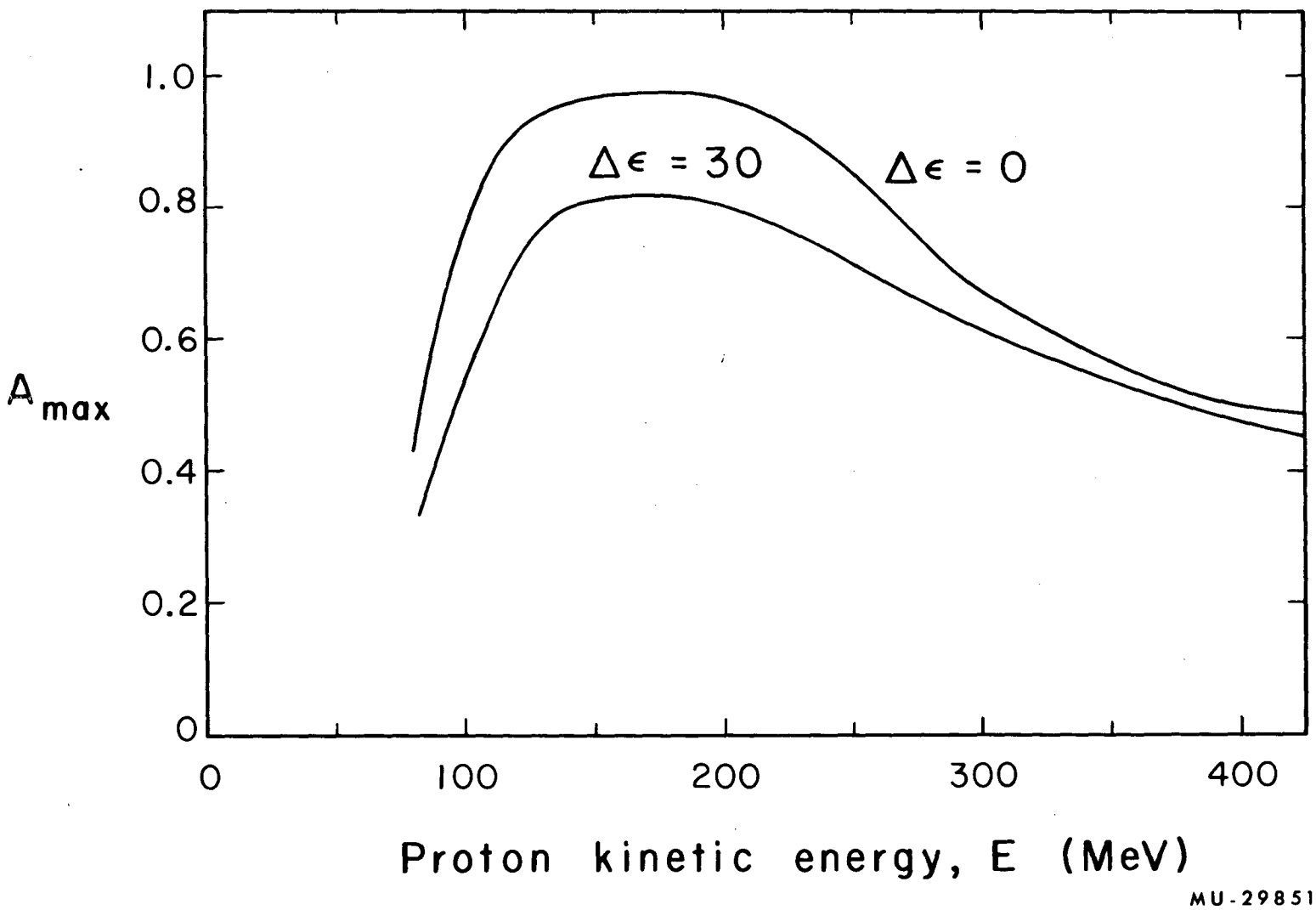
1.0
0.8
0.6
0.4
0.2
0
A_{max}
$\Delta\epsilon = 30$
$\Delta\epsilon = 0$
0
100
200
300
400
Proton kinetic energy, E (MeV)
MU-29851

Fig. 3.

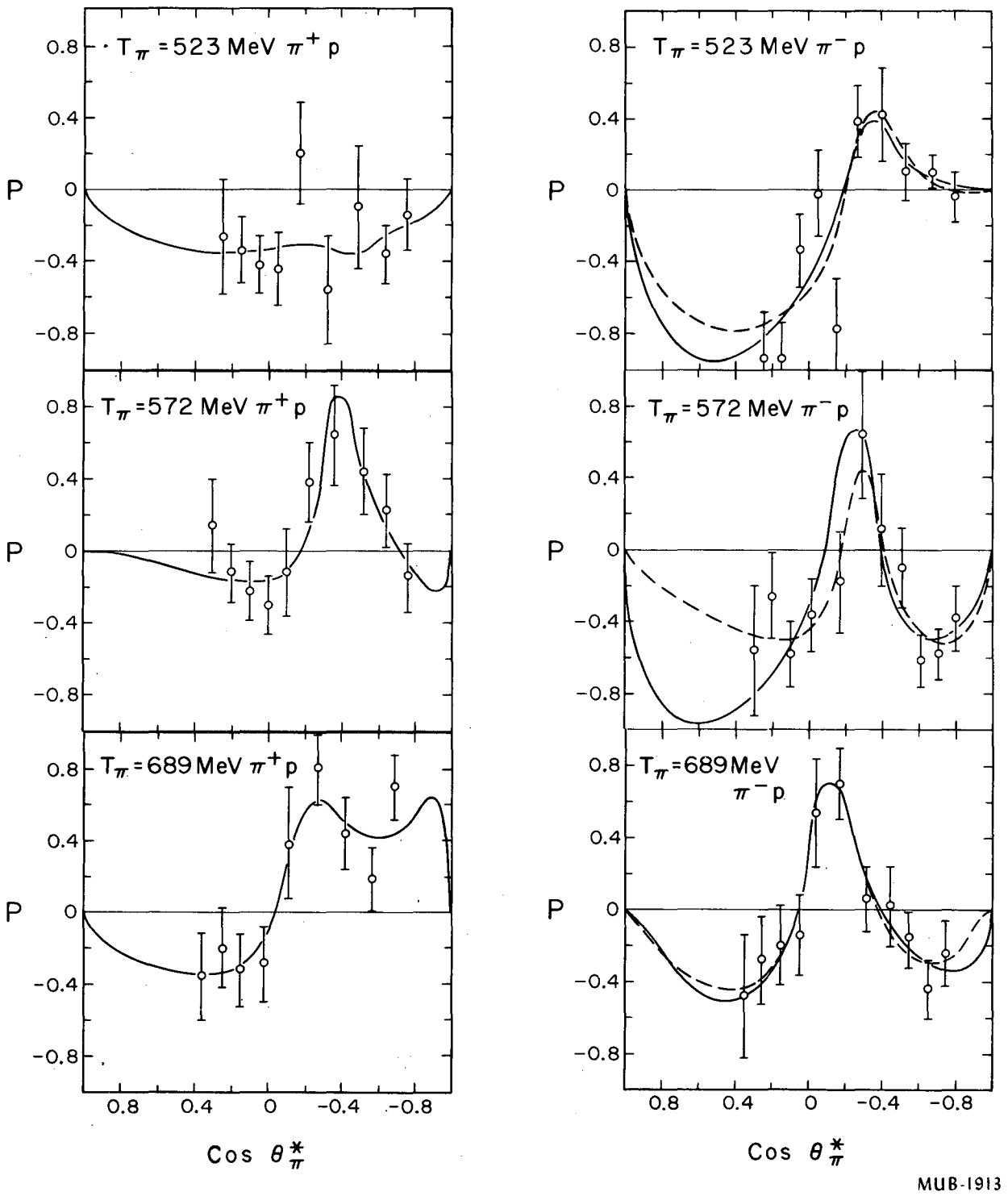
T_π = 523 MeV π^+ p
T_π = 523 MeV π^- p
T_π = 572 MeV π^+ p
T_π = 572 MeV π^- p
T_π = 689 MeV π^+ p
T_π = 689 MeV π^- p
P
0.8
0.4
0
-0.4
-0.8
Cos θ^*_π
MUB-1913

Fig. 4.

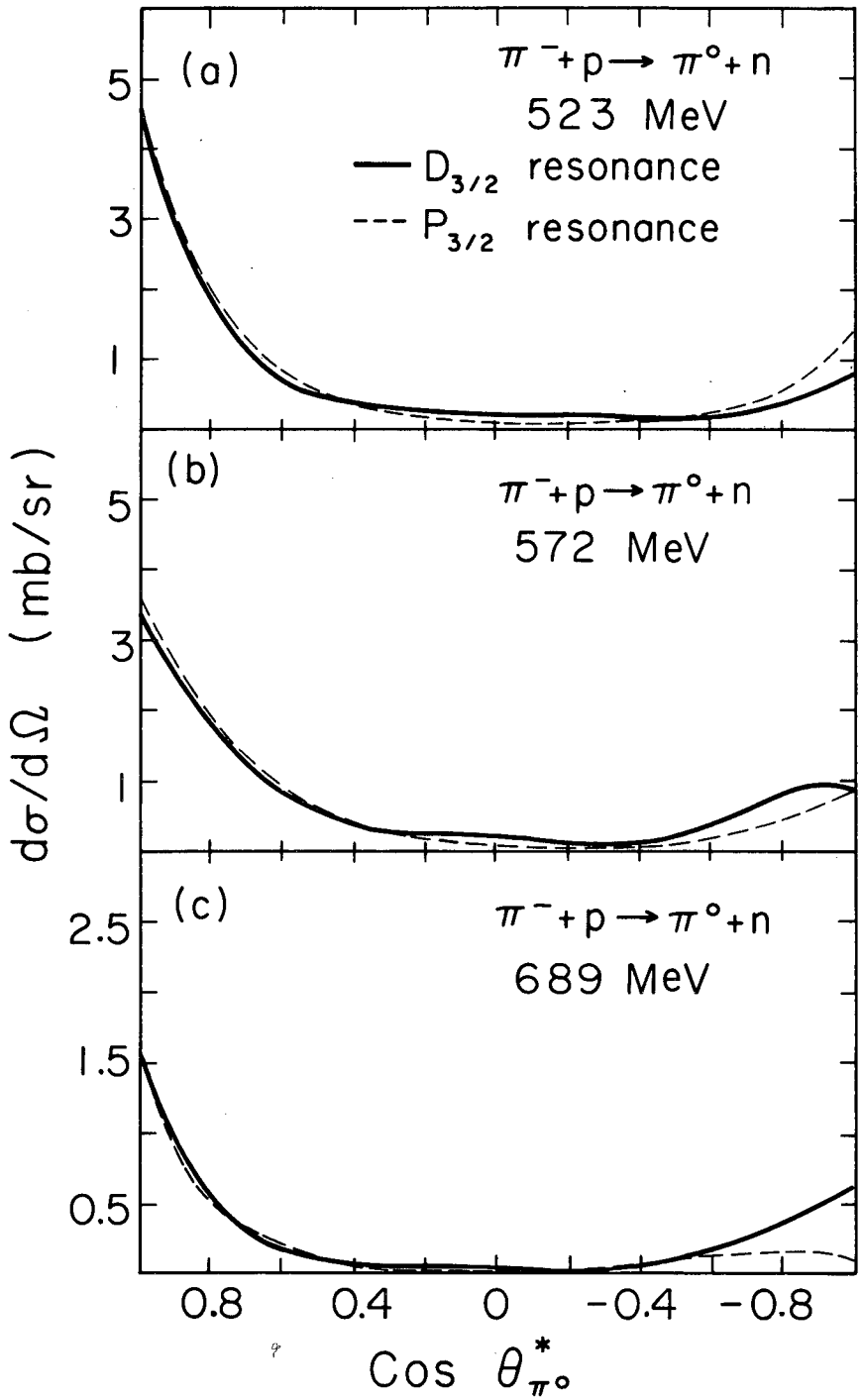
(a)
$\pi^- + p \rightarrow \pi^0 + n$
523 MeV
$D_{3/2}$ resonance
$P_{3/2}$ resonance
(b)
$\pi^- + p \rightarrow \pi^0 + n$
572 MeV
(c)
$\pi^- + p \rightarrow \pi^0 + n$
689 MeV
$d\sigma/d\Omega$ (mb/sr)
5
3
1
2.5
1.5
0.5
0.8
0.4
0
-0.4
-0.8
Cos $\theta^*_{\pi^0}$
MUB-2494

Fig. 5.

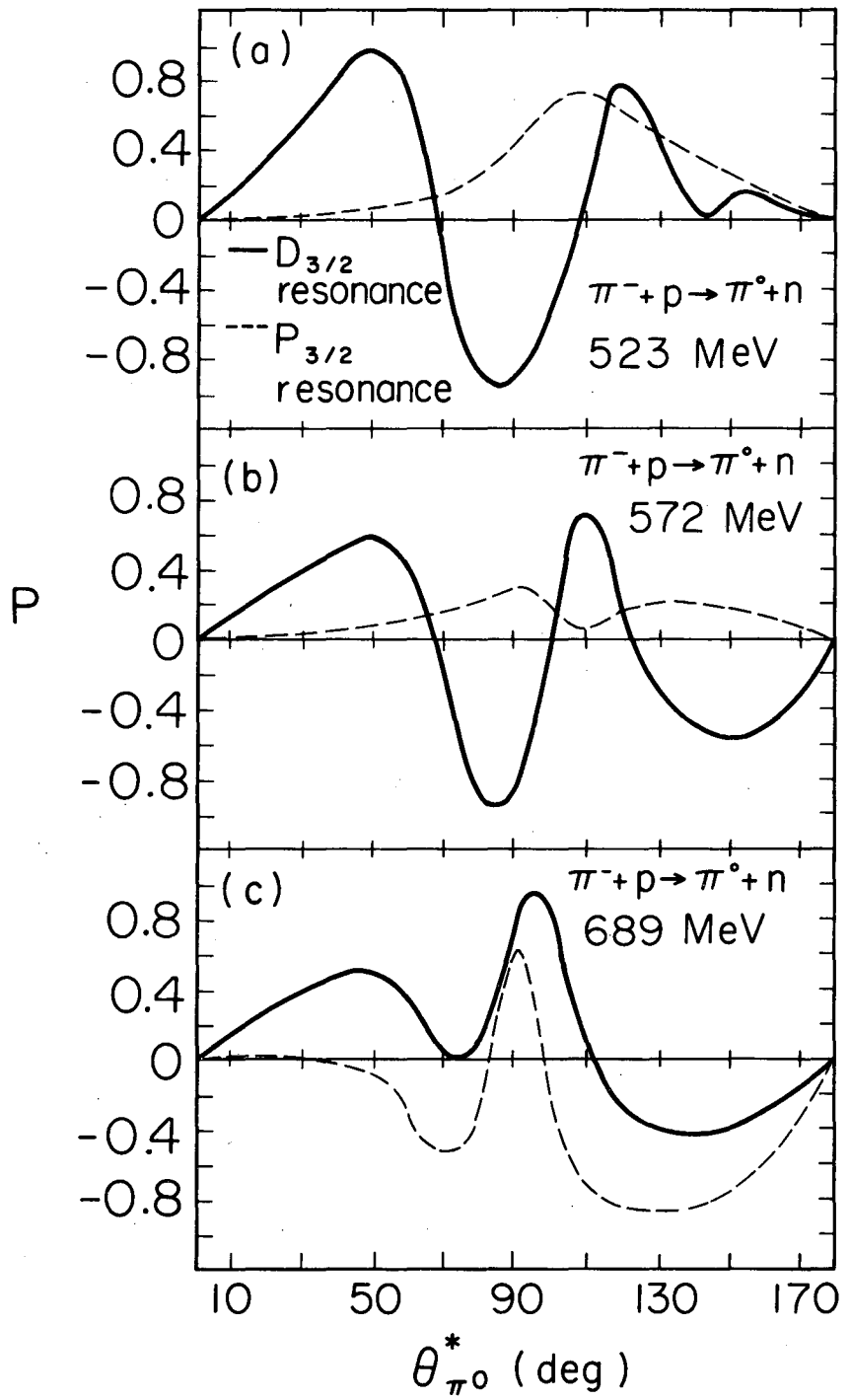

MUB-2493

Fig. 6

This report was prepared as an account of Government sponsored work. Neither the United States, nor the Commission, nor any person acting on behalf of the Commission:

A. Makes any warranty or representation, expressed or implied, with respect to the accuracy, completeness, or usefulness of the information contained in this report, or that the use of any information, apparatus, method, or process disclosed in this report may not infringe privately owned rights; or

B. Assumes any liabilities with respect to the use of, or for damages resulting from the use of any information, apparatus, method, or process disclosed in this report.

As used in the above, "person acting on behalf of the Commission" includes any employee or contractor of the Commission, or employee of such contractor, to the extent that such employee or contractor of the Commission, or employee of such contractor prepares, disseminates, or provides access to, any information pursuant to his employment or contract with the Commission, or his employment with such contractor.